

See discussions, stats, and author profiles for this publication at: <https://www.researchgate.net/publication/255617414>

# K in clinopyroxene at high pressure and temperature: An experimental study

Article in *American Mineralogist* · March 1997

DOI: 10.2138/am-1997-3-403

---

CITATIONS

142

---

READS

107

1 author:



[George E. Harlow](#)

American Museum of Natural History

184 PUBLICATIONS 5,306 CITATIONS

[SEE PROFILE](#)

Some of the authors of this publication are also working on these related projects:



Mineral Classification [View project](#)



Serpentinite Melanges in the Guatemala Suture Zone [View project](#)

## K in clinopyroxene at high pressure and temperature: An experimental study

GEORGE E. HARLOW

Department of Earth and Planetary Sciences, American Museum of Natural History,  
New York, New York 10024-5192, U.S.A.

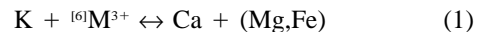
### ABSTRACT

Clinopyroxene (Cpx) is a principal upper-mantle phase for concentrating large cations but has not been viewed as a major crystal-chemical reservoir for K because  $K^+$  is considered too large to enter the largest site, M2, in the pyroxene structure. Accumulating data from high-pressure conditions indicate this inference is incorrect, so multianvil experiments have been performed to evaluate maximal K solubility in Cpx at high pressure. End members and mixtures of diopside, jadeite, and kosmochlor have been mixed with  $K_2CO_3$ ,  $KHCO_3$  or both in welded platinum capsules and heated typically for 24 h in the range of 5 to 14 GPa and 1200 to 1700 °C. These experiments produced K-rich Cpx in solid solutions by means of a fictive Kcpx component ( $KCrSi_2O_6$  or  $KAlSi_2O_6$ ). The maximum  $K_2O$  content obtained is 4.7 wt% in a Cpx ( $Di_{38}Ko_{39}Kcpx_{22}En_1$ ) formed from a 50:50 Di + Ko mixture at 10 GPa, 1400 °C. K uptake and partitioning is dependent positively on  $P$ , complexly on Cpx composition but not demonstrably on  $T$ .  $^{Cpx/liq}D_{K_2O}$  is in the range of 0.03–0.1 and  $^{Cpx/liq}D_{Na_2O}$  varies from 0.5 to 5, although the variations for each with Cpx composition are different. In diopside, Kcpx increases are always accompanied by increases in Nacpx, and cooperative Nacpx solution is necessary for Kcpx solution in the compositional systems examined. K appears to be accommodated in the M2 site of the Cpx structure by two types of spatial averaging: a large average M2 site, as in the case of Di, ameliorates the fit, but local accommodation by size averaging with a smaller M2 occupant, presumably Na, appears necessary, suggesting that the polyhedral compressibility of Na and K are large in comparison with Ca. In application to Cpx inclusions in diamond, the data here imply that a chromium diopside with ~1 wt%  $K_2O$  forms in the presence of a C-rich melt with 15–28 wt%  $K_2O$ .

### INTRODUCTION

Cpx, an important mineral of the upper mantle and crust, was not considered a major reservoir for K because the preponderance of compositional data for pyroxenes of all kinds show only trace K content. The crystal-chemical reasoning is that  $K^+$  [ $R(^{80}K^+) = 1.51 \text{ \AA}$ ; Shannon 1976] is too large to enter the largest site, M2, in the pyroxene structure. Harlow and Veblen (1991) have shown that  $K^+$  at levels of at least 0.07 cations per 6 O atoms (1.5 wt%  $K_2O$ ) can reside in the crystal structure of Cpx included in diamond and, thus, have confirmed the accuracy of some analyses of mantle Cpx with substantial  $K_2O$  (Prinz et al. 1975, McCandless and Gurney 1989, Rickard et al. 1989, Sobolev et al. 1991a) and more recently in Cpx inclusions from ultradeep [or ultra-high pressure (UHP)] metamorphic rocks (Sobolev et al. 1991b, 1994). Harlow and Veblen (1991) reasoned that high pressure and a K-rich environment were required to yield the K-rich pyroxenes found in diamonds. Because diopside, with a cell volume ( $V_c$ ) of ~439  $\text{\AA}^3$ , has larger average M2 (and M1) coordination polyhedra than omphacite ( $V_c = \sim 425 \text{ \AA}^3$ ) or particularly jadeite ( $V_c = \sim 401 \text{ \AA}^3$ ), they reasoned diopside should be a better host for K. However, for re-

placement of Ca by K a coupled exchange to balance charge such as



is required and observed in all natural samples. Because the cell volume and size of the M2 coordination polyhedron also increases with increasing M1 site occupant (Oberti and Caporuscio 1991; Cameron and Papike 1980), Harlow and Veblen (1991) proposed that K uptake should be favored in solid solutions incorporating a relatively large trivalent M1 cation, such as  $Cr^{3+}$ . These predictions have needed experimental testing.

Recently, long after the pioneering work of Shimizu (1971), a few experimental studies have produced K-rich Cpx at high pressure, e.g., Doroshev et al. (1992), Harlow (1992), Luth (1992), Edgar and Vukadinovic (1993). Here are reported experiments designed to yield maximum  $K_2O$  content in Cpx otherwise in the diopside-jadeite-kosmochlor (-enstatite) field. The goals also include testing the above mentioned hypotheses and examining the partition coefficients, pyroxene crystal-chemistry, and phase assemblages in a Cpx-potassium carbonate system.

TABLE 1. Microprobe analyses of pyroxene starting materials

	Weight percent oxides				
	1	2	3	4	5
SiO <sub>2</sub>	55.50	59.31	59.61	53.53	60.42
TiO <sub>2</sub>	0.03	0.02	0.01	0.06	0.00
Al <sub>2</sub> O <sub>3</sub>	0.04	1.10	0.44	0.00	25.39
Cr <sub>2</sub> O <sub>3</sub>	0.00	0.01	0.04	33.56	0.00
Fe <sub>2</sub> O <sub>3</sub> *	0.08	0.00	0.22	0.15	0.12
FeO	0.04	0.21	0.00	0.00	0.12
MnO	0.02	0.02	0.01	0.00	0.02
MgO	18.60	39.40	40.11	0.00	0.06
CaO	26.00	0.00	0.00	0.04	0.20
Na <sub>2</sub> O	0.03	0.01	0.01	13.72	15.45
K <sub>2</sub> O	0.00	0.00	0.00	0.00	0.00
Total	100.34	100.09	100.45	101.06	101.54
	<b>Cations for 6 atoms</b>				
Si	1.996	1.982	1.986	2.001	2.00
<sup>41</sup> Al	0.002	0.018	0.014	0.000	0.000
SUM T	1.997	2.000	2.000	2.001	2.00
Ti	0.001	0.000	0.000	0.002	0.000
<sup>61</sup> Al	0.000	0.025	0.003	0.000	0.99
Cr	0.000	0.000	0.001	0.992	0.000
Fe <sup>3+</sup> *	0.002	0.000	0.006	0.004	0.003
Fe	0.001	0.006	0.000	0.000	0.003
Mn	0.001	0.001	0.000	0.000	0.000
Mg	0.997	1.963	1.992	0.000	0.003
Ca	1.002	0.000	0.000	0.002	0.007
Na	0.002	0.001	0.001	0.994	0.99
K	0.000	0.000	0.000	0.000	0.000
Total	4.003	3.997	4.003	3.996	4.00

Notes: 1 is 39849, Wakefield Di; 2 is 100634, Zabargad Hi-Al En; 3 is 100634, Zabargad Low-Al En; 4 is Synthetic Kosmochlor; 5 is 33399 Manzanal Jd.

\* Fe<sup>3+</sup> determined by cation sum and charge balancing.

## MATERIALS, EXPERIMENTAL TECHNIQUE, AND ANALYSIS

### Materials

Starting materials in the experiments were mixtures of ground reagent SiO<sub>2</sub>, pyroxenes (most grains ≤100 mesh), K<sub>2</sub>CO<sub>3</sub>, or KHCO<sub>3</sub>. Carbonates were chosen as a K source because of their low melting temperature and their potential importance as components in some diamond-forming environments (Navon et al. 1987). Experiments involved exchanging K between carbonate and pyroxene on the Di-Jd and Di-Ko joins (either as solid solution or mixtures). Some experiments included small amounts of En, to examine minor Di-En solution on K uptake, and silica was added to one set of experiments at the suggestion of J.R. Smyth to avoid subsilicic (<2 Si per 6 O) Cpx. Natural pyroxene samples include diopside (AMNH 39849, Wakefield, Quebec, Canada), jadeite (AMNH 33399, Manzanal, Guatemala), and enstatite (AMNH 100634, Zabargad Island, Egypt). Kosmochlor was synthesized in a procedure intermediate to that of Ikeda and Yagi (1972) and Frondel and Klein (1965), where a sodium chromium silicate glass was ground and crystallized at 800 °C for 96 h in a muffle furnace (see Table 1 for analyses).

### High-pressure experimental procedure

Experiments were performed in multianvil apparatus using 600–2000 ton presses in the laboratory at Lamont

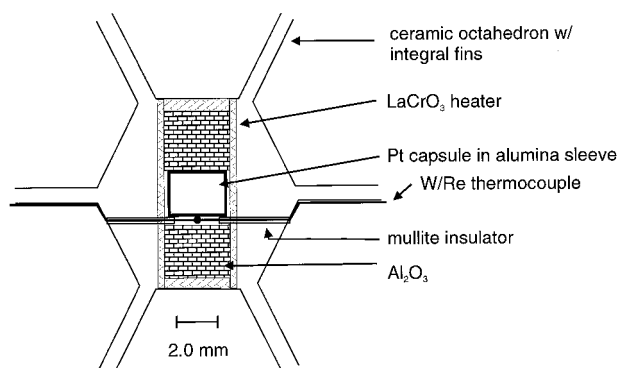


FIGURE 1. Drawing showing our latest experimental multianvil setup of octahedral assembly with LaCrO<sub>3</sub> heater, platinum capsule and off-set Tc at its base.

Doherty Earth Observatory, following the uniaxial design of Walker et al. (1990) and Walker (1991). Truncated tungsten carbide cubes in the assembly were both 25 and 16 mm in dimension, the latter employing tool-steel shims to match the assembly size of the former. The pressure-medium octahedra, to match cubes with 6 or 8 mm truncated edge lengths, were made of fired castable ceramic with integral fin gaskets and drilled for insertion of a solid cylindrical LaCrO<sub>3</sub> heater with a ~3.18 mm I.D. Potassium-carbonate is extremely reactive and mobile, so it must be encapsulated with other reactants in platinum capsules. Approximately 20 mg total of Cpx + K<sub>2</sub>CO<sub>3</sub> in equal amounts were packed into a cylindrical platinum capsule and dried for 20 min at ~150 °C before welding the capsule. Experiments with KHCO<sub>3</sub> were not dried because the intent was to add H<sub>2</sub>O to enhance reaction and diffusion rates. The capsule with an alumina liner was placed in contact with a D-type (W3%Re/W25%Re) transversely mounted thermocouple (Tc) so that the central hot-spot was ~1 mm away in the bottom of the capsule (see Fig. 1). Experiments using two thermocouples, one at the center of the assembly and the other at the far end of the capsule, have measured gradients of ~ ≤200 °C with the central Tc at 1700 °C. Consequently, the Tc temperature at 1 mm below center is estimated to be 50° below the hottest point in the capsule and is comparable to the average temperature in the capsule; the total gradient in the capsule is 100 °C. Experiments were brought up to *P*, then brought up to *T*, kept at a temperature for normally 24 h, then quenched, and finally depressurized. Some experiments were superheated by ~100° for 1 h before lowering to the final temperature. Other aspects of the experimental procedure, including pressure calibration that is considered accurate to ± 1/4 GPa, are similar to those described by Johnson and Walker (1993) and Walker (1991). Conditions for experiments cited here are given in Table 2.

### Analytical technique

Processed octahedral assemblies were imbedded in epoxy and sawn in half with a 4 mil diamond blade. One

TABLE 2. Conditions for experiments

	P(GPa)	T(°C)	Duration(h)	Phases	Experiment
				<b>Di<sub>86</sub>Ko<sub>9</sub>Qtz<sub>5</sub><sup>+</sup></b>	
K <sub>2</sub> CO <sub>3</sub>	5	<1500	29	Cpx, uvar, mgchr, glass	GG404
K <sub>2</sub> CO <sub>3</sub>	6	1400	23	Cpx, uvar, mgchr, glass	BB330
K <sub>2</sub> CO <sub>3</sub>	7	1500	24	Cpx, uvar, esk, glass	BB109
K <sub>2</sub> CO <sub>3</sub>	9	<1700	9	Cpx, uvar, glass	BB243
KHCO <sub>3</sub>	10	>1200	25	Cpx, K-wad, devit. glass	BB206
K <sub>2</sub> CO <sub>3</sub> *	10	1500	24	Cpx, K-wad, devit. glass	BB470
K <sub>2</sub> CO <sub>3</sub>	10	1500	21	Cpx, devit. glass	GG477
K <sub>2</sub> CO <sub>3</sub> **	11	1500	14	Cpx, KMgSil, Fo, glass	GG307
K <sub>2</sub> CO <sub>3</sub>	11	1700	24	Cpx, devit. glass or carb	GG299
K <sub>2</sub> CO <sub>3</sub>	12	1500	45	Cpx, esk, devit. glass or carb	BB85
K <sub>2</sub> CO <sub>3</sub>	14	1500	26	Cpx, devit. glass or card	BB89
				<b>Jd<sup>+</sup></b>	
K <sub>2</sub> CO <sub>3</sub>	11	1300	100	Cpx, carb	GG229
K <sub>2</sub> CO <sub>3</sub>	10	1500	24	Cpx, carb, glass	GG405
				<b>Ko<sup>+</sup></b>	
K <sub>2</sub> CO <sub>3</sub>	11	1300	24	Cpx, carb	GG227
K <sub>2</sub> CO <sub>3</sub>	10	1500	27	Cpx, K-wad, esk, KSiCr <sub>3</sub> O <sub>7</sub> , carb, glass?	GG415
				<b>Di<sub>50</sub>Jd<sub>50</sub><sup>+</sup></b>	
K <sub>2</sub> CO <sub>3</sub>	10	1500	26	Cpx, K-wad, carb	GG416
KHCO <sub>3</sub> + K <sub>2</sub> CO <sub>3</sub>	10	<1400	14	Cpx, K-cym?, carb	BB308
KHCO <sub>3</sub> + K <sub>2</sub> CO <sub>3</sub> *	10	1450	26	Cpx, glasses	GG499
KHCO <sub>3</sub> + K <sub>2</sub> CO <sub>3</sub> *	11	1450	24	Cpx, glasses	GG568
				<b>Di<sub>50</sub>Ko<sub>50</sub><sup>+</sup></b>	
K <sub>2</sub> CO <sub>3</sub> **	10	1450	24	Cpx, K-wad, esk, carb	GG486
K <sub>2</sub> CO <sub>3</sub>	10	1500	24	Cpx, K-wad, KSiCr <sub>3</sub> O <sub>7</sub> , glass, carb	GG412
KHCO <sub>3</sub> + K <sub>2</sub> CO <sub>3</sub>	10	1400	21	Cpx, K-wad, esk, carb	GG421
KHCO <sub>3</sub>	11	1500	22	Cpx, K-wad, esk, glass	TT48
				<b>Di<sub>70</sub>Ko<sub>20</sub>En<sub>20</sub><sup>+</sup></b>	
KHCO <sub>3</sub>	10	1300	24	Cpx, K-wad, KMgCrsil, carb	BB211
K <sub>2</sub> CO <sub>3</sub>	11	1400	27	Cpx, K-wad, KMgCrsil, uvar, glass	GG389

Notes: carb = carbonate, esk = Cr<sub>2</sub>O<sub>3</sub>, K-cym = KAlSi<sub>3</sub>O<sub>8</sub> · H<sub>2</sub>O, K-wad = K<sub>2</sub>Si<sub>4</sub>O<sub>9</sub>, KMgCrsil = new KMgCr-silicate, mgchr = Mg<sub>2</sub>CrO<sub>4</sub>, uvar = uvarovite, devit = devitrified.

\* Temperature was higher by 50° for the first hour; > or < indicates that, based on the final geometry (e.g., Tc position or compaction texture of the LaCrO<sub>3</sub> heater as not symmetrical) the appropriate capsule temperature may be higher or lower (probably by ≤ 50°).

\*\* Temperature was higher by 100° for the first hour.

half of each experiment was polished on diamond-impregnated laps with mineral spirits or oil for study of textures and compositions. The other half was kept in reserve for X-ray diffraction and ATEM/HRTEM analysis. Samples were stored in a drying oven at 60 °C, however, unless embedded in epoxy the carbonate phases eventually hydrate and effloresce. The polished samples were observed in incident and reflected light and imaged using a Zeiss DSM950 SEM with BSE and Link AN100 EDS. Microprobe analysis was carried out for constituent major elements except C and O using an upgraded ARL-SEMQ operating at 15 kV and 12.5 nA sample current. Natural minerals were used as standards, and the CIT-ZAF correction scheme according to Armstrong (1989) was employed. A focused beam was used for all phases except devitrified glasses and fine-grained carbonate for which a 5–10 μm beam was traversed for > 10 spots across the sample. Corrections for unanalyzed CO<sub>2</sub> and H<sub>2</sub>O were made by adding a specified missing quantity (in the proportion of carbonate and bicarbonate used in the charge) to the average of a group of analyses so that the adjusted average total equaled 100% (having taken everything into account in the ZAF correction).

## RESULTS

Cpx and glass or carbonate, are the dominant products, although other phases occur in minor amounts (Table 2). Phase segregation by thermal compaction (Leshner and Walker 1988) is conspicuous and common because of thermal gradients in the capsules. Carbonate or melt seeks the hot sides of the charge, and Cpx (and other crystalline phases) seek the colder center and ends (Figs. 2 and 3a); whereas an hourglass thermal profile should be expected in the capsule, inconsistent electrical properties of our LaCrO<sub>3</sub> result in variable compaction geometries. K-rich Cpx forms as overgrowths and recrystallizations, which was inferred from sharp compositional boundaries of overgrowth K-rich Cpx on relict cores and from compaction texture (Fig. 4). In some experiments, Cpx forms either tooth-shaped protuberances into carbonate (akin to feldspars in pegmatites), usually when compaction is incomplete, or new prisms extending from Pt or compacted Cpx into glass or carbonate, probably because of decreasing temperature or pressure creep from thermal pressure in the hydraulic system. In some experiments, there are immiscible carbonate-rich and silica-rich glasses (e.g.,

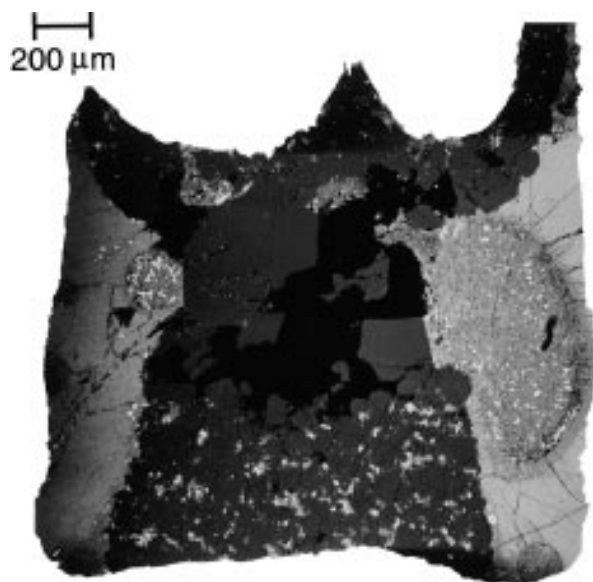


**FIGURE 2.** Texture of experiment GG405 (Jd +  $K_2CO_3$ ): Compaction and recrystallization of jadeite (dark gray) in center of capsule (black is epoxy, replacing plucked jadeite grains), finer unrecrystallized jadeite mixed with  $K_2CO_3$  at bottom, and formation of immiscible carbonate (devitrified blobs) and silicate liquids at hot sides of Pt capsule.

GG477 and GG405; Fig. 2), and in a mixed carbonate-bicarbonate experiment (GG499) a devitrified, void-rich sphere occurred in a silicate glass, presumably an immiscible carbonate-rich and  $H_2O$ -rich liquid. A result of larger thermal gradients and total Cpx recrystallization is thermally induced composition profiles (see Fig. 3). The generally smooth boundary between melt and carbonate and Cpx is an isotherm, and compositions were measured, if possible, adjacent to this boundary. Compositional data for glasses, carbonate, and non-Cpx phases will be reported in a separate treatment of the solubility characteristics and solution modeling.

The other crystalline experimental products typically exhibit distinctive habits: eskolaite ( $Cr_2O_3$ ) forms hexagonal plates, garnet forms dodecahedra, potassium-wadeite ( $K_2Si_4O_9$ ) and forsterite form rhombic prisms or blebs, magnesiochromite and  $KSiCr_3O_7$  forms blebs, and a phase with the formula  $K_{12-x}Mg_{11+2x}(Cr,Al)_{2-x}Si_{14}O_{48}$  forms a boundary between Cpx and glass (complete information on new phases will be reported elsewhere).

### K in Cpx

These experiments have produced K contents in Cpx exceeding amounts previously cited, and the compositions of Cpx products are appropriate to pyroxene crystal chemistry. K enrichments are measurable under all conditions attempted except when no potential balancing  $M1^{3+}$  cation is present, further substantiating pyroxene stoichiometry. The cation totals are invariably 4 per 6 O atoms, suggesting no vacancies, even in the H-bearing experiments, and K + Na is balanced by  $^{60}Al$  + Cr (Fig.

3c). Tetrahedral substitution of Si by Cr is not observed, but some Al substitution occurs at higher temperatures (GG416 in Table 3). Maximum content achieved so far is  $\sim 4.7$  wt%  $K_2O$  at 10 GPa in GG412 and GG421 (see Tables 3 and 4) with a molar Kcpx component of 22% [here Kcpx =  $KCrSi_2O_6$  but in general it will be used to represent  $K(Cr \text{ or } Al)Si_2O_6$ ]. Whereas high-resolution transmission electron microscopy has not as yet been conducted on products, several X-ray diffraction studies (on GG421 and TT48) by both powder and single-crystal methods show only sharp diffractions of  $C2/c$  Cpx without any other diffraction artifacts or phases. Results of these diffraction studies including structures will be presented elsewhere.

Experiments with  $K_2CO_3$  produce the greatest K enrichments in Cpx for a given  $P$  and  $T$  simply because of partitioning response, but these compositions are usually restricted to rims on unreacted starting crystals. Higher temperature experiments produce greater recrystallization (and melting and carbonate-silicate liquid immiscibility) but lower K content in the Cpx (in part because of dilution of  $K_2O$  in the increased volume of melt and carbonate). Addition of H by means of  $KHCO_3$  to the charge produces large ( $> 100 \mu m$ ) homogeneous Cpx crystals, probably in response to increased fluxing and recrystallization, but maximum K content can be diminished by the dilution of K in the carbonate.

Several important features of K uptake in Cpx are evident from the experiments. First, K uptake depends on the composition of Cpx involved, which appears to reflect the role of cell volume, in part. This aspect is clearest with the isomorphous exchanges of  $KNa_{-1}$  in jadeite and kosmochlor; in experiments at comparable conditions (GG415 and GG405) the level of K is two to three times greater in kosmochlor, with the larger  $V_c$  ( $\sim 419$  vs.  $\sim 401 \text{ \AA}^3$ ) and M1 polyhedron ( $10.55$  vs.  $9.37 \text{ \AA}^3$ ), than in jadeite. Second, however, in the Cpx mixtures studied here, maximum K uptake occurs in intermediate solid solutions of Di-Jd or Di-Ko rather than in compositions closer to diopside, which should have greater  $V_c$ . Third, Kcpx solution into diopside is accompanied by Jd or Ko solution in a sympathetic but not necessarily correlated manner (Na:K $\neq$ 1:1 or some other fixed ratio; see Fig. 3d and Table 4). These last two observations suggest (1) an average structure effect, that is some amelioration of fitting K into the crystal by mixing Na on the M2 site or Al or Cr and Mg on the M1 site or (2) deficit volume of mixing along the Di-Jd or Di-Ko join at high  $P$ . As for this latter possibility, data at ambient conditions for Di-Jd solid solutions (Rossi et al. 1983) show no departure from ideal mixing. Finally, a major problem in interpreting K-uptake  $P$ ,  $T$  systematics for diopsidic Cpx is the compositional effect (describe above); local recrystallization of admixed pyroxenes yields different Di contents and thus different Kcpx as well. Nevertheless the data demonstrate (most persuasively for the  $Di_{86}Ko_9Qtz_5 + K_2CO_3$  experiments and Cpx with about the same Di content, see Table 4) that K uptake, and perhaps partitioning, is dependent positively on  $P$ . The dependence

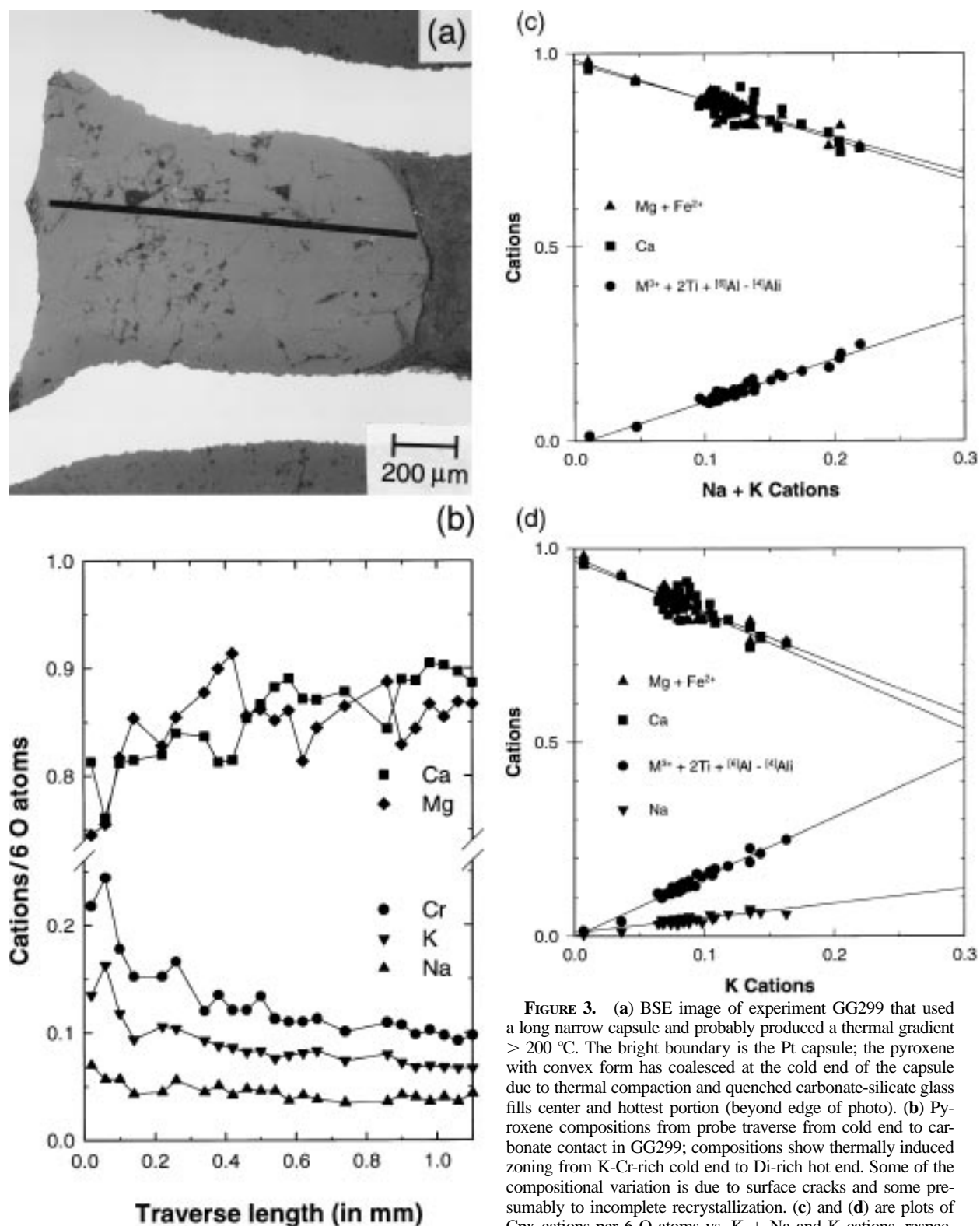


**FIGURE 3.** (a) BSE image of experiment GG299 that used a long narrow capsule and probably produced a thermal gradient  $> 200$  °C. The bright boundary is the Pt capsule; the pyroxene with convex form has coalesced at the cold end of the capsule due to thermal compaction and quenched carbonate-silicate glass fills center and hottest portion (beyond edge of photo). (b) Pyroxene compositions from probe traverse from cold end to carbonate contact in GG299; compositions show thermally induced zoning from K-Cr-rich cold end to Di-rich hot end. Some of the compositional variation is due to surface cracks and some presumably to incomplete recrystallization. (c) and (d) are plots of Cpx cations per 6 O atoms vs. K + Na and K cations, respectively, for a complete suite of analyses on GG299 Cpx. The term  $M^{3+} + 2Ti + [6]Al - [4]Al$  (where  $M^{3+} = Cr^{3+} + Fe^{3+}$ ) represents the charge balancing cation sum to balance the alkalis if Cpx crystal chemistry is to be maintained. Regression lines shown in (c) show good agreement with ideal stoichiometry.

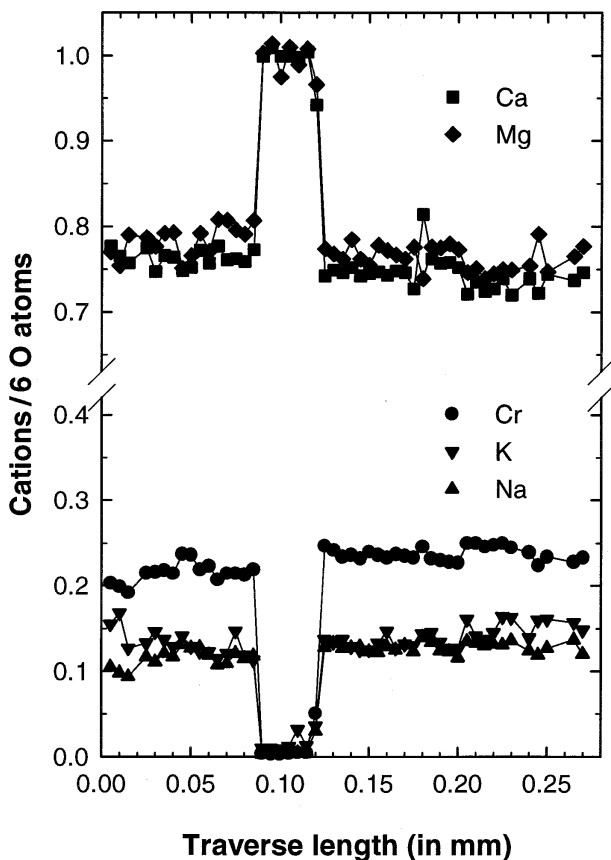


FIGURE 4. Pyroxene composition profile across a single grain showing the sharp boundary between Di core and Ko- + Kcpx overgrowth in experiment GG389.

on  $T$  is unclear from most of these experiments largely because of a lack of  $T$  variation among the data (which is in turn due to minimal reaction kinetics at lower  $T$  and excessive melting at high  $T$ ) and in some part because of a lower  $T$  accuracy from gradients and Tc junction variations. The thermal diffuse zoning in GG299 and a few comparisons among the data argue for K uptake depending inversely on  $T$ .

The average structure effect has been observed in a natural K-rich Cpx ( $\text{Ca}_{0.80}\text{K}_{0.073}\text{Na}_{0.023}\text{Mg}_{0.95}\text{Fe}_{0.06}\text{Cr}_{0.07}\text{Al}_{0.02}\text{Si}_{1.99}\text{O}_6$ ; Harlow 1996), an inclusion in a Koffiefontein diamond. In the average structure of this Cpx, 10% (Fe + Mg) in M2 (with radii 0.92 and 0.89 Å, respectively) balances the 7% K (with radius 1.51 Å) yielding an average M2 polyhedron only slightly larger than in diopside, 25.89 vs. 25.76 Å<sup>3</sup>, respectively. Moreover, the substitution of Fe + Mg into M2 is charge balanced in M1 by Mg, which is larger than Al or Cr, improving the fit for large occupants in M2 further (see Harlow 1996). Experiments with the mixture  $\text{Di}_{70} + \text{Ko}_{20} + \text{En}_{10}$  were conducted to reproduce similar Cpx, but a new KMgCr silicate and K-rich Cpx without any significant En content resulted. Nonetheless, if this kind of effect operates in the

experimental K-rich Cpx of intermediate Na-Ca composition, Mg is not the size-averaging cation.

### Partitioning

Another purpose of these experiments is to estimate the partitioning between K-rich media and K-Cpx as a minor component in Di-Jd or Di-Ko solid solutions appropriate to the formation of K-rich Cpx in diamonds and, indeed, other environments. K has always been treated as a trace element in Cpx, with a silicate melt partition coefficient,  $D_{\text{Cpx/liq}}^{\text{K}}$ , in the range of  $10^{-4}$  at low pressure to  $10^{-2}$  at 2–3 GPa (Hart and Dunn 1993; Shimizu 1974). The results here (Table 4) show that  $D_{\text{Cpx/liq}}^{\text{K}}$  (for an admittedly carbonate-rich melt) is greater at high pressure than previously measured and, from the few coexisting immiscible carbonate and silicate melts, it is generally greater than  $D_{\text{Cpx/carb}}^{\text{K}}$ . Moreover, generally the data demonstrate  $D_{\text{K}}$  is a function of Cpx composition. There is not a systematic relationship for  $D$  with the K<sub>2</sub>O content of the glass-carbonate or for any single group of experiments. Strictly, the data indicate that there is a maximum saturated Kcpx content in a particular pyroxene at a given  $P$  and  $T$  in the experiments, whereas the K content of the glass-carbonate varies according to bulk composition and the phase assemblage. The plateau of  $D$  values, particularly in the intermediate Di-Nacpx, indicates the maximum for  $D$  is near 0.1 at 10 GPa and 1500 °C. However, the Cpx solutions are actually controlled by components, so a more complex formulation is necessary, particularly for the complex Di-Ko-K<sub>2</sub>CO<sub>3</sub> system, and is the subject of further examination. Finally, the data also demonstrate the nearly compatible nature of Na in diopsidic Cpx with  $D_{\text{Cpx/liq}}^{\text{Na}}$  values between ~0.5 and 1, but Na is compatible in more sodic Cpx when values of  $D$  reach values of about 10 in jadeite. Again,  $D_{\text{Na}}$  varies with the composition of the Cpx.

### DISCUSSION

An essential issue in this study is the mechanism of solubility of K in Cpx that is enabled by high pressure. The effects of high pressure on crystal chemistry are usually viewed in terms of phase transformations in which coordination number increases, such as <sup>14</sup>Al (in albite) → <sup>6</sup>Al (in jadeite) or <sup>14</sup>Si (in pyroxene) → <sup>6</sup>Si (in silicate perovskite). It is not surprising that observations of K in Cpx from mantle xenoliths were viewed skeptically. Many of such samples were shown to contain exsolved and contaminant K-rich phases, and the coordination number of K in Cpx (presumably 8–7) is not larger than in the contaminant phases (14–12 in phlogopite; 9–8 in sanidine). However, a less well-studied relationship of crystal chemistry and pressure is differential ionic or polyhedral compressibility as it affects substitutions. Larger, lower-charge (low field strength-low FS) ions have relatively greater polyhedral compressibility in comparison with smaller, higher charge (high FS) ions (Hazen and Finger 1982; Hazen 1988) and generally greater linear bond compressibility (Kudoh et al. 1992 and Table 5

TABLE 3. Microprobe analyses of experimentally produced K-rich pyroxene

	Weight percent oxides									
	1	2	3	4	5	6	7	8	9	10
SiO <sub>2</sub>	55.53	54.29	53.96	59.68	53.30	55.21	57.48	52.94	53.03	54.92
TiO <sub>2</sub>	0.04	0.00	0.01	0.00	0.00	0.02	0.00	0.01	0.00	0.05
Al <sub>2</sub> O <sub>3</sub>	0.11	0.00	0.15	24.93	0.17	11.25	13.37	0.09	0.14	0.38
Cr <sub>2</sub> O <sub>3</sub>	3.44	6.10	6.80	0.01	34.05	0.01	0.00	17.92	19.45	8.85
Fe <sub>2</sub> O <sub>3</sub> *	0.18	0.03	0.18	0.18	0.00	0.08	0.02	0.00	0.00	0.00
FeO	0.00	0.00	0.00	0.07	0.00	0.00	0.00	0.00	0.00	0.00
MgO	16.95	14.82	14.20	0.19	0.05	10.72	9.06	8.57	7.96	13.94
CaO	22.87	20.49	19.66	0.35	0.02	14.57	12.59	10.90	10.18	18.43
Na <sub>2</sub> O	0.60	0.80	0.99	14.42	12.72	4.35	6.23	4.74	4.95	1.73
K <sub>2</sub> O	1.58	2.50	3.09	1.09	1.56	3.10	2.60	4.39	4.51	3.13
Total	101.30	99.04	99.05	100.92	101.87	99.32	101.35	99.57	100.22	101.44
<b>Cations for 6 oxygen atoms</b>										
Si	1.996	2.007	2.003	2.000	1.990	1.969	1.990	1.996	1.991	1.993
<sup>[4]</sup> Al	0.004	0.000	0.000	0.000	0.008	0.031	0.010	0.004	0.006	0.007
SUM T	2.000	2.007	2.003	2.000	1.998	2.000	2.000	2.000	1.997	2.000
Ti	0.001	0.000	0.000	0.000	0.000	0.000	0.000	0.000	0.000	0.001
<sup>[6]</sup> Al	0.000	0.000	0.007	0.985	0.000	0.442	0.536	0.000	0.000	0.010
Cr	0.098	0.178	0.200	0.000	1.005	0.000	0.000	0.534	0.577	0.254
Fe <sup>3+*</sup>	0.005	0.001	0.005	0.005	0.000	0.002	0.000	0.000	0.000	0.000
Fe	0.000	0.000	0.000	0.002	0.000	0.000	0.000	0.000	0.000	0.000
Mg	0.908	0.817	0.786	0.009	0.003	0.570	0.467	0.482	0.445	0.755
Ca	0.881	0.812	0.782	0.013	0.001	0.557	0.467	0.440	0.410	0.717
Na	0.042	0.057	0.071	0.937	0.920	0.301	0.418	0.346	0.360	0.122
K	0.072	0.118	0.147	0.047	0.074	0.141	0.115	0.211	0.216	0.145
Total	4.007	3.991	4.000	3.997	4.001	4.014	4.004	4.014	4.006	4.003

Notes: Values are for an individual analysis that is typical (within 1 S.D.) for a group of at least 6 analyses. 1. BB470: Di+Ko+Qtz+Kc, 1500 C, 10 GPa. 2. GG299: Di+Ko+Qtz+Kc, 1700 C, 11 GPa. 3. BB89: Di+Ko+Qtz+Kc, 1500 C, 14 GPa. 4. GG405: Jd+Kc, 1500, 10 GPa. 5. GG415: Ko+Kc, 1500, 10 GPa. 6. GG416: Di<sub>50</sub>Jd<sub>50</sub>+Kc, 1500 C, 10 GPa. 7. GG499: Di<sub>50</sub>Jd<sub>50</sub>+Kc+Kbc, 1450 C, 10 GPa. 8. GG412: Di<sub>50</sub>Ko<sub>50</sub>+Kc, 1500 C, 10 GPa. 9. GG421: Di<sub>50</sub>Ko<sub>50</sub>+Kc+Kbc, 1400 C, 10 GPa. 10. GG389: Di<sub>70</sub>Ko<sub>20</sub>En<sub>10</sub>+Kc, 1400 C, 11 GPa. Kc = K<sub>2</sub>CO<sub>3</sub>; Kbc = KHCO<sub>3</sub>.

\* Fe<sup>3+</sup> determined by cation sum and charge balancing.

where the interpretation has been extended to K<sup>+</sup> and Na<sup>+</sup>). The complete compressibility data for Cpx do not exist and predictions for structures as complex as in Cpx are, indeed, extrapolations. Nevertheless, the inference is that with increasing pressure a large ion like K<sup>+</sup> or Na<sup>+</sup> will behave more like relatively smaller ions Ca<sup>2+</sup> or Mg<sup>2+</sup>. Given sufficient charge-balancing trivalent cations, with increasing pressure the large ions should have increasing solubilities in Ca or Mg sites where the coordination number (in this case, 7–8 in the phases stable at high-*P*) is near or below the lower limit for the large ions at ambient conditions; temperature should have a reciprocal effect. The experimental data for Kcpx solution in Di, Jd, and Ko are consistent with differential compressibility based on polyhedral values in Table 5.

The experimental results may point to the significant compressibility of Na in Cpx by means of its role in Kcpx solubility in diopside. The size of K appears to be accommodated in the M2 site by spatial averaging in the only structure studied so far, as noted above, and Nacpx content varies sympathetically in diopsidic Cpx produced experimentally. Thus, a smaller Na<sup>+</sup> at high pressure would provide a mechanism of size averaging for K<sup>+</sup> to fit into M2 of diopside. Following this hypothesis, a limit is reached because the volume decrease due to Nacpx mixing in diopside ( $V_c \cong 439 \text{ \AA}^3$  for Di,  $401 \text{ \AA}^3$  for Jd, and  $419 \text{ \AA}^3$  for Ko) reduces the Kcpx solubility as compositions become dominated by Nacpx.

If Na<sup>+</sup> fulfills the accommodating role for Kcpx solu-

tion in Di at high pressure, Na<sup>+</sup> must be smaller than Ca<sup>2+</sup> at pressure. For tabulated radii at ambient conditions where Na<sup>+</sup> is larger than Ca<sup>2+</sup> (1.18 vs. 1.12 Å). The observed radii in Cpx at ambient conditions are more in line with the high pressure implications; the average M2-O bond lengths in Jd and Di at ambient conditions, 2.469 and 2.498 Å respectively (Cameron, et al. 1973), yield radii of 1.09 Å for Na<sup>+</sup> and 1.12 Å for Ca<sup>2+</sup> in coordination with <sup>[iv]</sup>O. Using these bond lengths from Cpx and values of  $\beta_c$  from Table 5, the calculated average bond lengths at 10 GPa are 2.389 Å for jadeite vs. 2.424 Å for diopside, only 0.006 Å greater than the difference at ambient conditions. The polyhedral compressibilities,  $\beta_p$ , indicate a much greater difference between the alkalis and Ca<sup>2+</sup>. The contrast in observed polyhedral volumes  $V_{p(0)}$  at ambient conditions and calculated values at 1500 °C and 10 GPa,  $V_{p(P,T)}$ , (see Table 5) could indicate both the size-accommodating behavior of Na at pressure and the greater compatibility of K in the M2 polyhedron of Cpx. However, actual configurations, bond lengths and polyhedral volumes, in high pressure structures of Nacpx and experimentally grown K-rich Cpx are needed to test these hypotheses.

These experimental results, which indicate that Kcpx content depends on high pressure and is correlated positively with *P* and perhaps negatively with *T* for a coexisting K-rich melt, can be compared with some data for natural Cpx. K contents in Cpx from diamonds where *P* > 5 GPa, *T* = 1000°–1400 °C (Harlow and Veblen 1991)



TABLE 4. Compositions and partition coefficients (*D*) for K<sub>2</sub>O and Na<sub>2</sub>O

Starting mixtures/ Cpx composition	<i>P</i> (GPa)	<i>T</i> (°C)	K <sub>2</sub> O (wt%)		Na <sub>2</sub> O (wt%)			Matrix	Experiment	
			Cpx	Carb or glass	Cpx	Carb or glass	<i>D</i> (Na <sub>2</sub> O)			
<b>Di<sub>86</sub>Ko<sub>9</sub>Qtz<sub>5</sub> + K<sub>2</sub>CO<sub>3</sub></b>										
Di <sub>86</sub> Ko <sub>9</sub> En <sub>4</sub> Kcpx <sub>4</sub>	5	<1500	0.9	18(1)	0.050	0.75	0.9(1)	0.83	glass	GG404
Di <sub>86</sub> Ko <sub>2</sub> Kcpx <sub>8</sub> En <sub>2</sub>	6	1400	0.9	11(1)	0.082	0.75	0.52(2)	1.4	glass	BB330
Di <sub>86</sub> Ko <sub>5</sub> Kcpx <sub>5</sub>	7	1500	1.0	28(3)	0.036	0.66	0.4(1)	1.7	glass	BB109
Di <sub>82</sub> Kcpx <sub>11</sub> Ko <sub>4</sub> En <sub>2</sub>	9	<1700	2.4	25(2)	0.096	0.55	0.9(1)	0.61	glass	BB243
Di <sub>72</sub> Ko <sub>12</sub> Kcpx <sub>11</sub> En <sub>2</sub> *	10	1200	2.5	37(2)	0.068	1.6	1.4(2)	1.1	carb	BB206
Di <sub>88</sub> Kcpx <sub>7</sub> Ko <sub>2</sub> En <sub>1</sub> **	10	1500	1.6	48(1)	0.033	0.6	1.7(1)	0.35	glass/carb	BB470
Di <sub>74</sub> Kcpx <sub>16</sub> Ko <sub>8</sub> En <sub>1</sub> **	10	1500	3.6	48(1)	0.075	1.1	1.7(1)	0.65	glass/carb	BB470
Di <sub>83</sub> Kcpx <sub>10</sub> Ko <sub>7</sub> En <sub>1</sub>	10	1500	2.1	30(3)	0.070	1.0	1.5(3)	0.67	glass/carb	GG477
Di <sub>83</sub> Kcpx <sub>8</sub> Ko <sub>4</sub> En <sub>3</sub> †	11	1500	1.8	36(2)	0.050	0.60	0.9(1)	0.67	devit glass	GG307
Di <sub>88</sub> Kcpx <sub>8</sub> Ko <sub>4</sub>	11	1700	1.7	37(1)	0.046	0.6	1.4(9)	0.43	devit glass	GG299
Di <sub>83</sub> Kcpx <sub>8</sub> Ko <sub>4</sub> En <sub>1</sub>	12	1500	1.7	34(3)	0.050	0.6	1.1(3)	0.55	devit glass	BB85
Di <sub>83</sub> Kcpx <sub>10</sub> Ko <sub>6</sub> En <sub>1</sub>	12	1500	2.2	34(3)	0.065	0.8	1.1(3)	0.73	devit glass	BB85
Di <sub>78</sub> Kcpx <sub>15</sub> Ko <sub>6</sub>	14	1500	3.2	51(2)	0.063	0.9	<0.02	45	devit glass	BB89
Di <sub>77</sub> Kcpx <sub>17</sub> Ko <sub>6</sub>	14	1500	3.5	51(2)	0.069	0.9	<0.02	45	devit glass	BB89
<b>Jd + K<sub>2</sub>CO<sub>3</sub></b>										
Jd <sub>99</sub> Kcpx <sub>1</sub>	11	1300	0.14	?		14.8	?		carb	GG229
Jd <sub>98</sub> Kcpx <sub>4</sub>	10	1500	1.0	46(2)	0.022	14.2	3.5(9)	4.1	carb	GG405
			1.0	26(1)	0.039	14.2	2.3(1)	6.2	glass	GG405
<b>Ko + K<sub>2</sub>CO<sub>3</sub></b>										
Ko <sub>96</sub> Kcpx <sub>4</sub>	11	1300	0.86	?		13.0	?		carb	GG227
Ko <sub>92</sub> Kcpx <sub>8</sub>	10	1500	1.6	57(3)	0.028	12.8	2.2(3)	5.8	carb	GG415
			1.6	44(2)	0.036	12.8	9.3(4)	1.4	glass?	GG415
<b>Di<sub>50</sub>Jd<sub>50</sub> + K<sub>2</sub>CO<sub>3</sub></b>										
Di <sub>53</sub> Jd <sub>31</sub> Kcpx <sub>13</sub> Ct <sub>3</sub> En <sub>1</sub>	10	1500	2.9	44(2)	0.066	4.5	3.6(4)	1.2	carb	GG416
Di <sub>4</sub> Jd <sub>90</sub> Kcpx <sub>6</sub>	10	1500	1.2	44(2)	0.027	13.5	3.6(4)	3.8	carb	GG416
<b>Di<sub>50</sub>Jd<sub>50</sub> + KHCO<sub>3</sub> + K<sub>2</sub>CO<sub>3</sub></b>										
Di <sub>48</sub> Jd <sub>37</sub> Kcpx <sub>8</sub> Ct <sub>4</sub> En <sub>2</sub>	10	<1400	1.9	62(2)	0.031	5.5	0.8(2)	6.9	carb	BB308
Di <sub>32</sub> Jd <sub>58</sub> Kcpx <sub>7</sub> Ct <sub>2</sub> En <sub>1</sub>	10	<1400	1.6	62(2)	0.026	8.6	0.8(2)	10.	carb	BB308
Di <sub>48</sub> Jd <sub>40</sub> Kcpx <sub>10</sub> Ct <sub>2</sub> †	10	1450	2.3	25(1)	0.092	6.0	2.0(1)	3.0	glass	GG499
Di <sub>56</sub> Jd <sub>36</sub> Kcpx <sub>8</sub> Ct <sub>1</sub> †	10	1450	1.2	33(1)	0.036	5.0	2.8(2)	1.8	glass	GG568
<b>Di<sub>50</sub>Ko<sub>50</sub> + K<sub>2</sub>CO<sub>3</sub> ± KHCO<sub>3</sub></b>										
Ko <sub>94</sub> Di <sub>23</sub> Kcpx <sub>12</sub> En <sub>1</sub> †	10	1450	2.4	33(2)	0.073	8.7	2.0(4)	4.4	glass	GG486
Di <sub>42</sub> Ko <sub>34</sub> Kcpx <sub>22</sub> En <sub>1</sub>	10	1500	4.6	53(1)	0.087	4.6	4.5(1)	1.0	carb	GG412
			4.6	40(3)	0.12	4.6	4.3(1)	1.1	glass	GG412
Di <sub>38</sub> Ko <sub>30</sub> Kcpx <sub>22</sub> En <sub>1</sub>	10	1400	4.7	51(2)	0.092	5.5	1.2(2)	4.6	carb	GG421
Ko <sub>95</sub> Di <sub>27</sub> Kcpx <sub>16</sub> En <sub>2</sub>	11	1500	3.2	39(2)	0.082	7.5	2.5(1)	3.0	glass	TT48
<b>Di<sub>70</sub>Ko<sub>20</sub>En<sub>10</sub> + K<sub>2</sub>CO<sub>3</sub> ± KHCO<sub>3</sub></b>										
Di <sub>72</sub> Kcpx <sub>16</sub> Ko <sub>13</sub>	11	1350	3.5	60(2)	0.058	1.8	0.8(2)	2.25	carb	GG389
Di <sub>71</sub> Kcpx <sub>14</sub> Ko <sub>13</sub>	11	1450	3.2	47(3)	0.068	1.8	2.0(3)	0.9	carb	GG389
Di <sub>70</sub> Ko <sub>12</sub> En <sub>2</sub> Kcpx <sub>16</sub>	10	1300	3.3	47(3)	0.062	1.7	1.6(3)	1.06	carb	BB211

Note: ? indicates that compositions could not be determined.

\* lone experiment using KHCO<sub>3</sub> instead of K<sub>2</sub>CO<sub>3</sub>.

\*\* Temperature was higher by 50° for the first hour; < and > as in Table 2.

† Temperature was higher by 100° for the first hour.

TABLE 5. Comparison of linear compressibilities and polyhedral compressibilities (Mbar<sup>-1</sup>)

	$\beta_e$	$\beta_o$	$\beta_p(O)$	$\beta_p(F)$	$\beta_p(Cpx)$	$\alpha_p$	$V_{p(0)}$	$V_{p(P,T)}$
Cr	0.14	0.14	0.43			1.69	10.51	10.31
Al	0.16	0.14	0.42			2.65	9.37	9.33
Mg	0.22	0.21	0.62–0.67	1.0	0.95	4.25	11.85	11.39
Ca	0.30	0.30	0.91–1.18	1.16	0.99	4.42	25.76	24.72
Na	0.33*		3.13	2.22	Jd	3.74	24.58	20.18
					Ko	3.50	25.36	20.75
K	0.30*		3.7	3.413		3.74	36.40	25.30

Notes:  $\beta_e$  = calculated linear bond compressibility and  $\beta_o$  = observed linear bond compressibility data from Kudoh et al. (1992);  $\beta_p(O)$  = polyhedral compressibility for various O polyhedra and  $\beta_p(F)$  = polyhedral compressibility for F in fluorides from Hazen and Finger (1982);  $\beta_p(Cpx)$  data: Di from Levien and Prewitt (1981);  $\alpha_p$  = polyhedral thermal expansivity for Cpx (Cameron et al. 1973) except K which is from Hazen and Finger (1982) for 8-fold coordination;  $V_{p(0)}$  = polyhedral volume in Cpx except for K for which the microcline value is used (Smyth and Bish 1988);  $V_{p(P,T)}$  = the calculated polyhedral volume at 1500 °C and 10 GPa using  $\alpha_p$  and  $\beta_p(Cpx)$  for Mg and Ca,  $\beta_p(O)$  for Cr & Al, and  $\beta_p(F)$  for K and Na (which are less than  $\beta_p(O)$  for Na and K).

\* The equation  $\beta_e = 0.217 [\Delta r/\Delta \log(z/n)]^2$  (Kudoh et al. 1992) was used with radii (*r*) from Shannon (1976).

range as high as 1.5 wt%  $K_2O$  in the  $Di_{80}$  Cpx noted above. K-rich diopside (1.1–1.5 wt%  $K_2O$ , foremost as  $Di_{88}Kcpx_5Jd_3Cts_2Fs_2$ ) is included in garnet grains from UHP metamorphic rocks from Kazakhstan with estimates of  $P = \sim 4$  GPa,  $T = \sim 1000$  °C, (Sobolev and Shatsky 1990; Sobolev et al. 1991b). These conditions are potentially subsolidus but in a very limited way show a similar relationship as these experiments.

Only limited prior experimental data exist for comparisons. Earlier experiments showed a small increase of K in diopside in synthetic basaltic melts containing between 1.2 and  $\sim 3$  wt%  $K_2O$  as an anhydrous or oxyphlogopite component:  $\leq 0.017$  wt%  $K_2O$  at 32 kbar and 1450 °C yielding  $D_{Cpx/liq}^{Cpx}$  of 0.0013 (Erlank and Kushiro 1970) and 0.26 wt%  $K_2O$  at 10 GPa and 1400 °C (Shimizu 1971). These values are very low compared with the data presented here, and the difference may be due to the absence of Na in the starting material. Thus even though Al is available for charge compensation of  $K^+$  in Cpx, the absence of Na in its perceived role as a size compensator in the M2 site may prevent the formation of K-enriched Cpx. Other experiments by Erlank and Kushiro (1970) using omphacite + anhydrous phlogopite or diopside + potassic richterite component at 24–25 kb and 1000 °C resulted in 50 ppm or less K in Cpx, in spite of the presence of Na in the Cpx (no compositions reported). It is possible that at 1000 °C the reactions were too sluggish or zones of K-rich Cpx too small to be observed.

The results of Edgar and Vukadinovic (1993) for Cpx in lamproite partial melt at 1200 to 1500 °C and 5 to 6 GPa are comparable to the results here. Maximum  $K_2O$  content of  $\sim 1.6$  wt%  $K_2O$  is produced at lowest  $T$  and highest  $P$  in  $Di_{57}Jd_{15-19}$  Cpx, and Kcpx content drops off simultaneously with increasing  $T$ , En content, and decreasing  $K_2O$  content of the coexisting melt. All these factors should tend to decrease Kcpx content based on the observations made here. The partition coefficients  $D_{Cpx/liq}^{Cpx}$  of Edgar and Vukadinovic (1993) show a somewhat higher maximum value, 0.19 at 1200 °C and 5 GPa, but the value decreases dramatically with increasing  $T$ . This highest value may represent a closer convergence of the melt composition to the optimum for Kcpx solution. The dramatic changes in  $D_{Cpx/liq}^{Cpx}$  in their experiments undoubtedly manifest the effect of the En content (decreased  $V_c$ ) of Cpx on its capacity to accept a Kcpx component. Consequently, their results appear consistent with those reported here but should only be applied to Cpx of the compositions they report.

Because Kcpx solid solution in diopsidic Cpx appears to depend on Nacpx solid solution as well, the pressure dependencies of Nacpx-Di miscibility are an important factor in the formation of K-rich Cpx. The pressure dependence of jadeite stability and Di-Jd solubility is well known (Gasparik 1985), such that low pressure formation of  $KAlSi_2O_6$  component in diopsidic Cpx is not expected. For conditions of high  $P/T$  metamorphism, recent data for metasomatic omphacite coexisting with

phengite formed at  $\sim 400$  °C and 6–10 kbar showed  $K_2O$  contents only at the detection limit,  $\sim 0.01$  wt% (and so were not reported in Harlow 1994), consistent with other data for comparable conditions. One infers that the values of  $D$  for omphacite-phengite or omphacite-K-feldspar are much lower at these conditions than for Cpx-melt or Cpx-carbonate at 10 GPa:  $10^{-3}$  vs.  $10^{-1}$ . Kosmochlor-diopside solutions may be a better subject for lower pressure evaluation as kosmochlor is stable at ambient pressure even though such Cpx is restricted to mantle xenoliths and rare metasomatic high  $P/T$  environments (Harlow and Olds 1987). Unfortunately, the experimental data for the Di-Ko system are contradictory. Partial miscibility of Ko in Di is reported by Ikeda and Yagi (1972) at 1 ATM, a maximum content of  $Ko_{23.1}$  at 1140 °C (probably as low as 1050 °C) that decreases upon increasing  $T$ . On the other hand, complete miscibility is reported by Yoder and Kullerud (1970) at 0.2 GPa, and yet Vredevoogd and Forbes (1975) state that Ko solubility decreases substantially below 1 bar values at 2 GPa and that Di is insoluble in Ko. Di-Ko solubility may be nearly complete at 10 GPa and 1500 °C, on the basis of observations presented here. Clarifications are required in the Ko-Di system before inferences can be made about  $KCrSi_2O_6$  component solubility in diopside-rich members at lower pressures.

#### IMPLICATIONS FOR THE MANTLE

These results show that diopsidic pyroxene may be more useful for measuring the K content in the mantle than K-rich minerals. Mica and amphibole appropriate to mantle composition are not stable at high  $P$ ; they undergo major coordination-changing or dehydration reactions with depth in the mantle, breaking down between 30 and 200 km (1–6 GPa at 1000 to 1300 °C; Sudo and Tatsumi 1990). Potassium-feldspar is a stable host for K only up to  $\sim 7$  GPa and 1500 °C (Yagi et al. 1994) and was found only rarely in eclogitic xenoliths and diamond inclusions (Schulze and Helmstaedt 1988). The higher pressure phases  $K_2Si_4O_9$ , wadeite and  $KAlSi_5O_8$  hollandite are stable at high  $P$  but have never been recovered in natural samples. Whereas K-rich phases may be exceedingly rare or absent (or missed in thin section) in typical mantle rocks, Cpx is not likely to be missed, may be the fundamental solid host for K in most of the upper mantle, and should be a very good monitor of K activity in the mantle.

The values of  $D_{Cpx/liq}^{Cpx}$  measured here, although reflecting an unusual composition, can be used along with the data of Edgar and Vukadinovic (1993) to put some limits on K contents in coexisting liquids. K-rich Cpx found as inclusions in diamonds results from high pressure and high K activity: the data here imply that a diopside with  $\sim 1$  wt%  $K_2O$  forms in the presence of a C-rich melt-fluid with 14 to 33 wt%  $K_2O$ ; for omphacite a slightly less  $K_2O$ -rich melt-fluid would be needed. Very K-rich environments are indicated for these Cpx found in diamonds.

## ACKNOWLEDGMENTS

I am particularly grateful and indebted to Dave Walker who invited me into his lab to test my hypotheses and who is always generous with advice and wit. Krikitt Johnson has been helpful with advice and critiques, and Damon Winter served as an excellent intern during two summers, getting the hang of multi-anvil artistry and my idiosyncrasies. The manuscript was improved by reviews of D. Walker, J.R. Smyth and R.W. Luth. I gratefully acknowledge the National Science Foundation (EAR 93-14819) for support of this research.

## REFERENCES CITED

- Armstrong, J.M. (1989) CITZAF: Combined ZAF and phi-rho (Z) electron beam correction programs. California Institute of Technology, Pasadena, California.
- Cameron, M., and Papike, J.J. (1980) Crystal chemistry of silicate pyroxenes. In *Mineralogical Society of America Reviews in Mineralogy*, 7, 5–92.
- Cameron, M., Sueno, S., Prewitt, C.T., and Papike, J.J. (1973) High-temperature crystal chemistry of acmite, diopside, hedenbergite, jadeite, spodumene, and ureyite. *American Mineralogist*, 58, 594–618.
- Doroshev, A.M., Sobolev, N.V., and Brey, G. (1992) Experimental evidence of high-pressure origin of the potassium-bearing clinopyroxenes. *Proceedings of the International Geological Congress, Kyoto II*, 29th, 602.
- Edgar, A.D., and Vukadinovic, D. (1993) Potassium-rich clinopyroxene in the mantle: An experimental investigation of a K-rich lamproite up to 60 kbar. *Geochimica et Cosmochimica Acta*, 57, 5063–5072.
- Erlank, A.J., and Kushiro, I. (1970) Potassium contents of synthetic pyroxenes at high temperatures and pressures. *Carnegie Institution Year Book* 68, pp. 233–236.
- Frondel, C., and Klein, C., Jr. (1965) Ureyite,  $\text{NaCrSi}_2\text{O}_6$ : A new meteoritic pyroxene. *Science*, 149, 742–744.
- Gasparik, T. (1985) Experimentally determined compositions of diopside-jadeite pyroxene with albite and quartz at 1200–1350 °C and 15–34 kbar. *Geochimica et Cosmochimica Acta*, 49, 865–870.
- Harlow, G.E. (1992) Potassium in clinopyroxene at high pressure. *Geological Society of America Abstracts with Programs*, 24, A129.
- (1994) Jadeitites, albitites and related rocks from the Motagua Fault Zone, Guatemala. *Journal of Metamorphic Geology*, 12, 49–68.
- (1996) Structure refinement of a natural K-rich diopside: The effect of K on the average structure. *American Mineralogist*, 81, 632–638.
- Harlow, G.E., and Olds, E.P. (1987) Observations on terrestrial ureyite and ureyitic pyroxene. *American Mineralogist*, 72, 126–136.
- Harlow, G.E., and Veblen, D.R. (1991) Potassium in clinopyroxene inclusions from diamonds. *Science*, 251, 652–655.
- Hart, S.R., and Dunn, T. (1993) Experimental cpx/melt partitioning of 24 trace elements. *Contributions to Mineralogy and Petrology*, 113, 1–8.
- Hazen, R.M. (1988) A useful fiction: polyhedral modeling of mineral properties. *American Journal of Science*, 288-A, 242–269.
- Hazen, R.M., and Finger, L.W. (1982) Structural variations with pressure. In *Comparative Crystal Chemistry: Temperature Pressure, Composition, and the Variation of Crystal Structure*, p. 147–164. Wiley, New York.
- Hazen, R.M., and Prewitt, C.T. (1977) Effects of temperature and pressure on interatomic distances in oxygen-based minerals. *American Mineralogist*, 62, 309–315.
- Ikeda, K., and Yagi, K. (1972) Synthesis of kosmochlor and phase equilibria in the join  $\text{CaMgSi}_2\text{O}_6$ - $\text{NaCrSi}_2\text{O}_6$ . *Contributions to Mineralogy and Petrology*, 36, 63–72.
- Johnson, M., and Walker, D. (1993) Brucite  $[\text{Mg}(\text{OH})_2]$  dehydration and the molar volume of  $\text{H}_2\text{O}$  to 15 GPa. *American Mineralogist*, 78, 271–284.
- Kudoh, Y., Prewitt, C.T., Finger, L.W., and Ito, E. (1992) Ionic radius-bond strength systematics, ionic compressibilities and an application to  $(\text{Mg,Fe})\text{SiO}_3$  perovskites. In Y. Syono and M.H. Manghnani, Eds., *High-pressure research: applications to earth and planetary sciences*, p. 215–218. American Geophysical Union, Washington, D.C.
- Leshner, C., and Walker, D. (1988) Cumulate maturation and melt migration in a temperature gradient. *Journal of Geophysical Research*, 93, 10295–10311.
- Levien, L., and Prewitt, C.T. (1981) High-pressure structural study of diopside. *American Mineralogist*, 66, 315–323.
- Luth, R.W. (1992) Potassium in clinopyroxene at high pressure: Experimental constraints (abs.). *EOS*, 73, 608.
- McCandless, T.E., and Gurney, J.J. (1989) Sodium in garnet and potassium in clinopyroxene: Criteria for classifying mantle eclogites. In J. Ross et al., Eds., *Kimberlites and related rocks, vol. 2: Their mantle/crust setting, diamonds, and diamond exploration*. Geological Society of Australia Special Publication 14, p. 827–832. Blackwell Scientific Publications, Carlton, Victoria, Australia.
- Navon, O., Hutcheon, I.D., Rossman, G.R., and Wasserburg, G.J. (1987) Mantle-derived fluids in diamond micro-inclusions. *Nature*, 335, 784–789.
- Oberti, R., and Caporuscio, F.A. (1991) Crystal chemistry of clinopyroxenes from mantle eclogites: A study of the key role of the M2 site population by means of crystal-structure refinement. *American Mineralogist*, 76, 1141–1152.
- Prinz, M., Manson, D.V., Hlava, P.F., and Keil, K. (1975) Inclusions in diamonds: Garnet lherzolite and eclogite assemblages. In L. H. Ahrens, J. B. Dawson, A. R. Duncan and A. J. Erlank, Eds., *Physics and Chemistry of the Earth, vol. 9*, p. 797–815. Pergamon Press, Oxford, U.K.
- Rickard, R.S., Harris, J.W., Gurney, J.J., and Cardoso, P. (1989) Mineral inclusions in diamonds from the Koffiefontein Mine. In J. Ross et al., Eds., *Kimberlites and related rocks, vol. 2: Their mantle/crust setting, diamonds, and diamond exploration*. Geological Society of Australia Special Publication 14, p. 1054–1062. Blackwell Scientific Publications, Carlton, Victoria.
- Rossi, G., Smith, D.C., Ungaretti, L., and Domeneghetti, M.C. (1983) Crystal-chemistry and cation ordering in the system diopside-jadeite: a detailed study by crystal structure refinement. *Contributions to Mineralogy and Petrology*, 83, 247–258.
- Schulze, D.J., and Helmstaedt, H. (1988) Coesite-sanidine eclogites from kimberlite: products of mantle fractionation or subduction. *Journal of Geology*, 96, 453–443.
- Shannon, R.D. (1976) Revised effective ionic radii and systematic studies of interatomic distances in halides and chalcogenides. *Acta Crystallographica*, A32, 751–757.
- Shimizu, N. (1971) Potassium contents of synthetic clinopyroxenes at high pressures and temperatures. *Earth and Planetary Science Letters*, 11, 374–380.
- (1974) An experimental study of the partitioning of K, Rb, Cs, Sr and Ba between clinopyroxene and liquid at high pressures. *Geochimica et Cosmochimica Acta*, 38, 1789–1798.
- Smyth, J.R., and Bish, D.L. (1988) *Crystal structures and cation sites of the rock-forming minerals*, 332 p. Allen & Unwin, Boston.
- Sobolev, N.V., and Shatsky, V.S. (1990) Diamond inclusions in garnets from metamorphic rocks: a new environment for diamond formation. *Nature*, 343, 742–746.
- Sobolev, N.V., Barkumenko, I.T., Yefimova, E.S., and Pokhilenko, N.P. (1991a) Morphological features of microdiamonds, sodium in garnets and potassium in pyroxene from two eclogite xenoliths from Udachnaya kimberlite pipe, Yakutia. *Doklady Akademii Nauk SSSR*, 321, 585–592.
- Sobolev, N.V., Shatsky, V.S., and Vavilov, M.A. (1991b) Inclusions of microdiamonds and coexisting minerals in garnets and zircons from metamorphic rocks of Kokchetav Massif, USSR (abs.). *Terra*, 3, 83.
- Sobolev, N.V., Shatsky, V.S., Vavilov, M.A., and Goryainov, S.V. (1994) Zircons from ultra high pressure metamorphic rocks of folded regions as a unique container of inclusions of diamond, coesite and coexisting minerals. *Doklady Akademii Nauk*, 334, 488–492.
- Sudo, A., and Tatsumi, Y. (1990) Phlogopite and K-amphibole in the upper mantle: Implication for magma genesis in subduction zones. *Geophysical Research Letters*, 17, 29–32.
- Vredevoogd, J.J., and Forbes, W.C. (1975) The system diopside-ureyite at 20 kb. *Contributions to Mineralogy and Petrology*, 52, 147–156.
- Walker, D. (1991) Lubrication, gasketing, and precision multi-anvil experiments. *American Mineralogist*, 76, 1092–1100.

Walker, D., Carpenter, M.A., and Hitch, C.M. (1990) Some simplifications to multianvil devices for high pressure experiments. *American Mineralogist*, 75, 1020–1028.

Yagi, A., Suzuki, T., and Akaogi, M. (1994) High Pressure Transitions in the System  $\text{KAlSi}_3\text{O}_8$ - $\text{NaAlSi}_3\text{O}_8$ . *Physics and Chemistry of Minerals*, 21, 12–17.

Yoder, H.S.M., Jr., and Kullerud, G. (1970) Kosmochlor and the chromite plagioclase association. *Carnegie Institution of Washington Yearbook*, 69, 155–157.

MANUSCRIPT RECEIVED APRIL 26, 1996

MANUSCRIPT ACCEPTED DECEMBER 11, 1996